Available online at www.sciencedirect.com
ScienceDirect
Journal of Power Sources 175 (2008) 784–788
JOURNAL OF POWER SOURCES
www.elsevier.com/locate/jpowsour

Short communication

Carbon-supported Pd–Ir catalyst as anodic catalyst in direct formic acid fuel cell

Xin Wang [a], Yawen Tang [a], Ying Gao [b], Tianhong Lu [a,c,*]

[a] College of Chemistry and Environmental Science, Nanjing Normal University, Nanjing 210097, PR China
[b] Department of Chemistry, College of Physical and Chemistry, Harbin Normal University, Harbin 150080, PR China
[c] Changchun Institute of Applied Chemistry, Chinese Academy of Sciences, Changchun 130022, PR China

Received 29 August 2007; received in revised form 29 September 2007; accepted 1 October 2007
Available online 10 October 2007

Abstract

It was reported for the first time that the electrocatalytic activity of the Carbon-supported Pd–Ir (Pd–Ir/C) catalyst with the suitable atomic ratio of Pd and Ir for the oxidation of formic acid in the direct formic acid fuel cell (DFAFC) is better than that of the Carbon-supported Pd (Pd/C) catalyst, although Ir has no electrocatalytic activity for the oxidation of formic acid. The potential of the anodic peak of formic acid at the Pd–Ir/C catalyst electrode with the atomic ratio of Pd and Ir = 5:1 is 50 mV more negative than that and the peak current density is 13% higher than that at the Pd/C catalyst electrode. This is attributed to that Ir can promote the oxidation of formic acid at Pd through the direct pathway because Ir can decrease the adsorption strength of CO on Pd. However, when the content of Ir in the Pd–Ir/C catalyst is too high the electrocatalytic activity of the Pd–Ir/C catalyst would be decreased because Ir has no electrocatalytic activity for the oxidation of formic acid.

Keywords: Direct formic acid fuel cell; Carbon-supported Pd–Ir catalyst; Palladium; Iridium

1. Introduction

In the recent years, it has been recognized that the direct methanol fuel cell (DMFC) has some serious disadvantages [1]. Firstly, methanol is easy to penetrate through the Nafion membrane, causing the waste of methanol and the decrease in the DMFC performance. Secondly, the electrocatalytic activity of Pt usually used as the anodic catalyst in DMFC is low and Pt is easy to be poisoned with CO, an intermediate of the methanol oxidation. Thirdly, the use of methanol is not safe because methanol is a toxic, evaporable and burnable compound.

Recently, many advantages of DFAFC have been recognized [2–5]. For example, formic acid is non-toxic. The dilute formic acid is on the US Food and Drug Administration list of food additives [6]. It is not inflammable and thus its storage and transportation are safe. It has two orders of magnitude smaller crossover flux through a Nafion membrane than methanol [7]. When formic acid is used as the fuel in DFAFC the operation concentration can be as high as 20 M, while the best concentration of methanol in DMFC is only about 2 M [2,3]. Thus, the power density of DFAFC can be higher than that of DMFC, although the energy density of formic acid is only one-third that of methanol. Usually, the performance of DFAFC should be better than that of DMFC because the active energy of the oxidation of formic acid is smaller than that of the methanol oxidation. The electrooxidation performance of formic acid is better than that of methanol, because formic acid has the electronic motive force calculated from the Gibbs free energy higher than methanol [2].

It was reported that the electrooxidation of formic acid could undergo through two parallel pathways, the direct pathway and CO pathway [8–14]. In the direct pathway, formic acid is directly oxidized to CO_2.

$$HCOOH + Pt^0 \rightarrow CO_2 + 2H^+ + 2e^- \quad (1)$$

In the CO pathway, formic acid is firstly oxidized to form CO, an intermediate and then CO is oxidized to CO_2.

$$HCOOH + Pt^0 \rightarrow Pt\text{–}CO + H_2O \quad (2)$$

* Corresponding author at: College of Chemistry and Environmental Science, Nanjing Normal University, Nanjing 210097, PR China. Tel.: +86 25 83598031.
E-mail address: tianhonglu@263.net (T. Lu).

0378-7753/$ – see front matter © 2007 Elsevier B.V. All rights reserved.
doi:10.1016/j.jpowsour.2007.10.011

$$Pt^0 + H_2O \rightarrow Pt\text{–}OH + H^+ + e^- \quad (3)$$

$$Pt\text{–}CO + Pt\text{–}OH \rightarrow 2Pt^0 + CO_2 + H^+ + e^- \quad (4)$$

The overall reaction:

$$HCOOH \rightarrow CO_2 + 2H^+ + 2e^- \quad (5)$$

The previous studies have shown that the electrooxidation rate of formic acid at the Pt catalyst is insufficient for the practical application, because the electrooxidation of formic acid at the Pt catalyst is mainly through the CO pathway and thus Pt is easy to be poisoned by CO [15–19]. Recently, Masel and coworkers. [20,21] have discovered that the Pd and Pd/C catalysts can overcome the CO poisoning effect because the electrooxidation of formic acid at the Pd and Pd/C catalysts is mainly through the direct pathway. In order to further improve the electrocatalytic performance of the Pd and Pd/C catalysts, the Pd-based binary metallic catalysts have been investigated [22]. Until now, the mechanism of the increase in electrocatalytic performance of the Pd-based binary metallic catalysts is not very clear. Two hypotheses have been suggested [23]. It was considered that the second atom can increase the adsorption ability of the active oxygen and then the oxidation rate of formic acid or it can prevent from the formation of strongly adsorbed CO. The Pd-based binary metallic catalysts studied include Pd–Ni [24], Pd–Au [25], Pd–Pt [26], etc.

In this work, it was reported for the first time that the Pd–Ir/C catalyst showed the electrocatalytic activity for the oxidation of formic acid better than that of the Pd/C catalyst, although Ir has no electrocatalytic activity for the oxidation of formic acid. The reason for that Ir can increase the electrocatalytic activity of Pd for the oxidation of formic acid was discussed.

2. Experimental

The preparation method of the catalysts is as follows: 60 mg Vulcan XC-72 carbon, 1.10 mL 0.04504 M $PdCl_2$ and 2.3 mL 0.067 M $(NH_4)_2IrCl_6$ were added to 10 mL H_2O. Then, the suspension obtained was sonicated for 30 min and stirred mechanically for 4 h. After the pH of the suspension was adjusted to 8–9 with the NaOH solution, 10 mL 1.0 mg/mL $NaBH_4$ solution was added dropwise into the suspension to reduce $PdCl_2$ and $(NH_4)_2IrCl_6$. After the suspension was sonicated for 20 min, it was stirred for 1 h at 10 °C in order to make sure that $PdCl_2$ and $(NH_4)_2IrCl_6$ were completely reduced to Pd and Ir. Then, it was filtered and washed with triply distilled water and ethanol sequentially. Finally, it was dried in a vacuum oven at 60 °C for 12 h. The catalyst obtained is the Pd–Ir/C catalyst with 20 wt.% Pd–Ir and the atomic ratio of Pd:Ir = 1:1 and was noted as the Pd–Ir/C-1 catalyst.

The preparation method of other catalysts is similar to that mentioned above. Only the components of the initial suspension were different. For the Pd–Ir/C catalyst with 20 wt.% Pd–Ir and the atomic ratio of Pd:Ir = 3:1 noted as the Pd–Ir/C-3 catalyst, the components of the initial suspension were 60 mg Vulcan XC-72 carbon, 2.00 mL 0.04504 M $PdCl_2$ and 1.3 mL 0.067 M $(NH_4)_2IrCl_6$ in 10 mL H_2O. For the Pd–Ir/C catalyst with 20 wt.% Pd–Ir and the atomic ratio of Pd:Ir = 5:1 noted as the Pd–Ir/C-5 catalyst, the initial components of the suspension were 60 mg Vulcan XC-72 carbon, 2.30 mL 0.04504 M $PdCl_2$ and 1.00 mL 0.067 M $(NH_4)_2IrCl_6$ in 10 mL H_2O. For the Pd/C catalyst with 20 wt.% Pd, the initial components of the suspension were 60 mg Vulcan XC-72 carbon, 3.13 mL 0.04504 M $PdCl_2$ in 10 mL H_2O. For the Ir/C catalyst with 20 wt.% Ir, the initial components of the suspension were 60 mg Vulcan XC-72 carbon and 3.80 mL 0.067 M $(NH_4)_2IrCl_6$ in 10 mL H_2O.

The electrochemical measurements were performed with a CHI600 electrochemical analyzer and a conventional three-electrode electrochemical cell. A Pt plate was used as the auxiliary electrode. The saturated calomel electrode (SCE) electrode was used as the reference electrode. All the potentials were quoted with respect to SCE. The working electrode was prepared as follows. A glassy carbon electrode was polished with 0.3 and 0.05 μm Al_2O_3 sequentially and washed. Eight milligrams catalyst and 4 mL C_2H_5OH were mixed to obtain the catalyst slurry. Then, 8.9 μL slurry was spread on the surface of the glassy carbon electrode. After drying, 4.5 μL Nafion (5 wt.%) solution was covered on the surface of the catalyst layer and the working electrode was obtained. The diameter of the glassy carbon electrode is 4 mm and its apparent surface area was 0.1256 cm^2. The specific loading of Pd–Ir, Pd or Ir on the electrode surface was 28 μg cm^{-2}.

The solution for the electrochemical measurement was 0.5 M H_2SO_4 solution with or without 0.5 M HCOOH. N_2 was bubbled into the solution for 10 min to remove O_2 dissolved in the solution prior to the electrochemical measurements. In the process of the measurement, N_2 was flowed above the solution. For the electrochemical measurement of the adsorbed CO, when the electrode potential was fixed at 0 V CO was bubbled into the solution for 15 min until CO was fully adsorbed on the electrode. Then, N_2 was bubbled into the solution for 10 min to remove CO in the solution. All the electrochemical measurements were carried out at 30 ± 1 °C.

The composition of catalysts was determined using the energy dispersive spectrometer (EDS) with Vantage Digital Acquisition Engine (Thermo Noran, USA). The X-ray diffraction (XRD) measurements of catalysts were performed on Model D/max-rC diffractometer using Cu Kα radiation (λ = 0.15406 nm) and operating at 45 kV and 100 mA.

3. Results and discussion

Fig. 1 displays the EDS spectrum of the Pd–Ir/C-5 catalyst. The Pd and Ir peaks were observed except the carbon peak. The atomic ratio of Pd and Ir in the catalyst is 5.0:0.95, indicating that both $PdCl_2$ and $(NH_4)_2IrCl_6$ added have been completely reduced to Pd and Ir in the Pd–Ir-5 catalyst.

Fig. 2 shows the XRD patterns of the Pd/C and the different Pd–Ir/C catalysts. It was observed from Fig. 2, curve d that except the characteristic peak of carbon at 24.5°, the 2θ values of other four peaks are 40.07°, 46.53°, 68.19° and 82.02°. They correspond to the 2θ values of Pd(1 1 1), (2 0 0), (2 2 0) and (3 1 1) crystal faces of the face centered cubic crystalline of the Pd particles in the Pd/C catalyst, respectively, (ASTM standard 5-

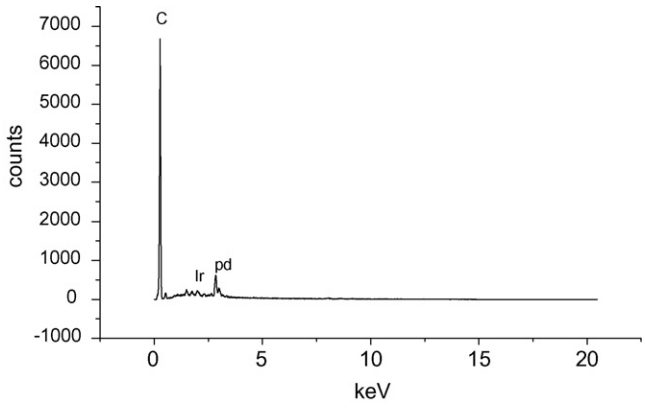

Fig. 1. The EDS spectrum of the Pd–Ir/C-5 catalyst.

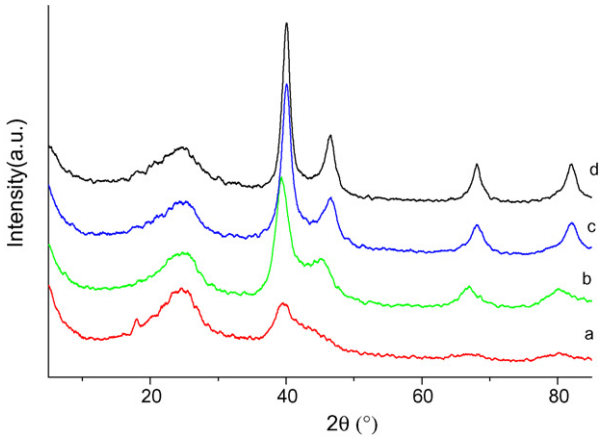

Fig. 2. The XRD patterns of (a) the Pd–Ir/C-1, (b) Pd–Ir/C-3, (c) Pd–Ir/C-5 and (d) Pd/C catalysts.

681(Pd)), illustrating that the Pd particles in the Pd/C catalyst possess the structure of the face centered cubic crystalline. The average sizes, relative crystallinity and lattice parameter of the Pd particles in the Pd/C catalyst were calculated to be 9.27, 2.90 and 0.6339 nm, respectively, according to the procedure in literatures [27–29]. The data of the average sizes, relative crystallinities and the lattice parameters of all the catalysts were listed in Table 1.

In the XRD pattern of the Pd–Ir/C-5 catalyst (Fig. 2, curve c), the 2θ values of four peaks of Pd are 40.05°, 46.52°, 68.06° and 82.00°, respectively, which are slightly smaller than that of the Pd/C catalyst. Furthermore, no peaks related to Ir were observed. This indicated that Ir has entered into the Pd lattice forming the Pd–Ir alloy. Due to that the radius of Ir atom is larger than that of Pd atom, the 2θ values of the Pd–Ir lattice in the Pd–Ir/C-5 catalyst are smaller than that of the Pd lattice in the Pd/C catalyst and the lattice parameter of Pd in the Pd–Ir/C-5 catalyst is larger than that of the Pd particles in the Pd/C catalyst. In addition, it was found the peaks of the Pd particles in the Pd/C catalyst are higher and sharper than that of the Pd–Ir particles in the Pd–Ir/C-5 catalyst, illustrating that the average size (6.72 nm) and relative crystallinity (1.76) of the Pd–Ir particles in the Pd–Ir/C-5 catalyst are smaller and lower than that of the Pd particles in the Pd/C catalyst, respectively. This illustrated that Ir can prevent from the aggregation of the particles because the preparation method of the catalysts is the same.

Table 1
The structure data of the catalysts obtained from the XRD measurements

Catalysts	Average size (nm)	Relative crystallinity	Lattice parameter (nm)
Pd/C	9.27	2.90	0.6339
Pd–Ir/C-1	2.59	0.86	0.6503
Pd–Ir/C-3	4.22	1.57	0.6478
Pd–Ir/C-5	6.72	1.76	0.6360

When the atomic ratio of Pd and Ir is decreased the 2θ values of four peaks of Pd are also decreased. For example, the 2θ values of four peaks of Pd of the Pd–Ir/C-3 catalyst are 39.29°, 45.11°, 66.89° and 80.09°, respectively (Fig. 2, curve b) and they are 39.04°, 45.01°, 66.55° and 80.00°, respectively, for the Pd–Ir/C-1 catalyst (Fig. 2, curve a). This illustrated that more Ir atoms have entered into the Pd lattice. Furthermore, the intensities and the sharpness extents of the peaks of Pd are decreased, indicating that the average size and relative crystallinity of the Pd–Ir particles in the catalysts are decreased (Table 1). This further demonstrated that Ir can prevent from the aggregation of the Pd particles.

Fig. 3 presents the cyclic voltammograms of 0.5 M H_2SO_4 solution at the different catalyst electrodes. Firstly, it can be observed from Fig. 3, curve e that there is almost no the adsorption/desorption peaks of hydrogen at the Ir/C catalyst electrode, illustrating that Ir is not active for the adsorption/desorption of hydrogen. Secondly, the charge–discharge current of the double-layer at the Pd–Ir/C-1 catalyst electrode is largest among all the catalyst electrodes (Fig. 3, curve a), because as mentioned above, the Pd–Ir/C-1 catalyst possesses the smallest average size of the metal particles and thus, the largest surface area among all the catalysts. Thirdly, the peaks of the adsorption/desorption of hydrogen around 0 V are obvious at the Pd/C catalyst electrode (Fig. 3, curve d). Because Pd possesses the excellent ability and Ir has the poor ability for the adsorption/desorption of hydrogen,

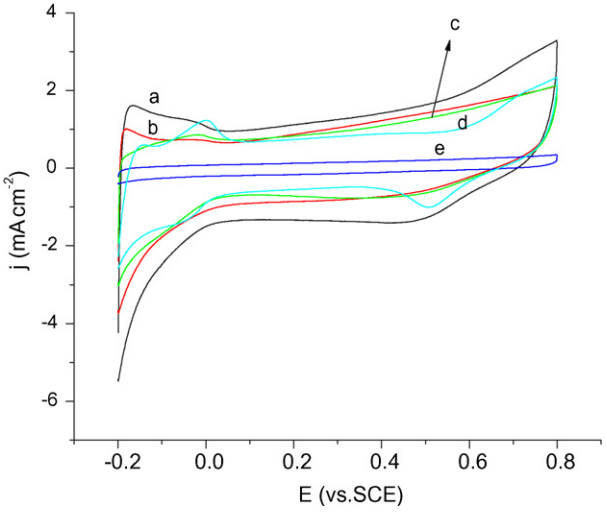

Fig. 3. The cyclic voltammograms of 0.5 M H_2SO_4 solution at (a) the Pd–Ir/C-1, (b) Pd–Ir/C-3, (c) Pd–Ir/C-5, (d) Pd/C and (e) Ir/C catalyst electrodes.

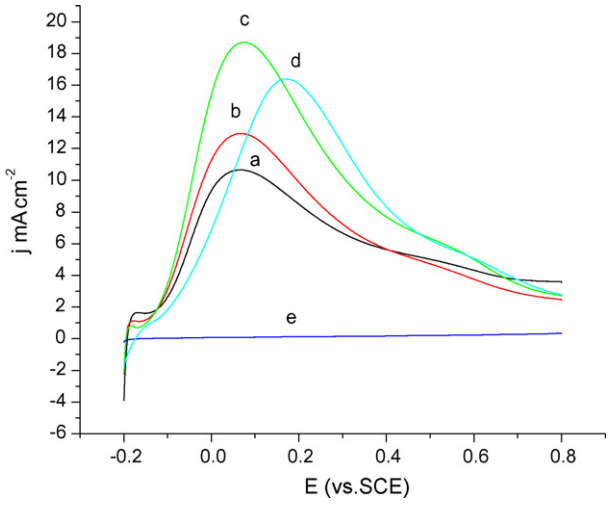

Fig. 4. The linear sweeping voltammograms of 0.5 M HCOOH in 0.5 M H_2SO_4 solution at (a) the Pd–Ir/C-1, (b) Pd–Ir/C-3, (c) Pd–Ir/C-5, (d) Pd/C and (e) Ir/C catalyst electrodes.

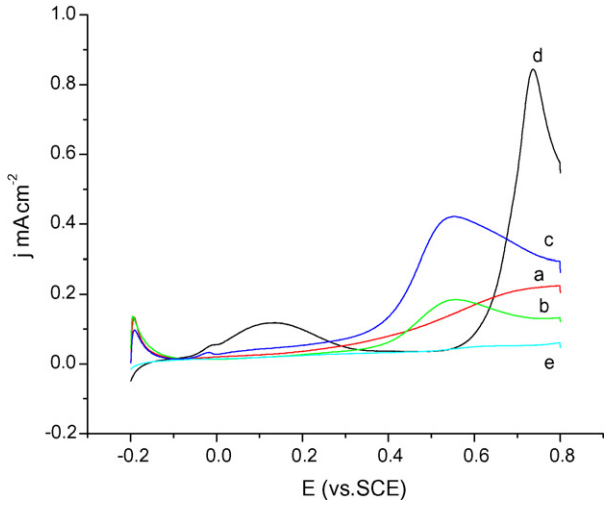

Fig. 5. The linear sweeping voltammograms of the adsorbed CO in 0.5 M H_2SO_4 solution at (a) the Pd–Ir/C-1, (b) Pd–Ir/C-3, (c) Pd–Ir/C-5, (d) Pd/C and (e) Ir/C catalyst electrodes.

the current densities of the peaks of the adsorption/desorption of hydrogen around 0 V are decreased according to the order of the Pd/C > Pd–Ir/C-5 > Pd–Ir/C-3 > Pd–Ir/C-1 > Ir/C catalyst electrode. Fourthly, the onset potentials of the Pd oxidation for all the Pd/C and Pd–Ir/C catalysts are at about 0.55 V and the reduction peaks are located at about 0.48 V.

Fig. 4 shows the linear sweeping voltammograms of 0.5 M HCOOH in 0.5 M H_2SO_4 solution at the different catalyst electrodes. Obviously, no anodic peak was observed at the Ir/C catalyst electrode (Fig. 4, curve e), indicating that the Ir/C catalyst has no electrocatalytic activity for the oxidation of formic acid. The anodic peaks at the Pd/C catalyst electrode are located at 0.12 and about 0.5 V. The corresponding peak current densities are 16.62 and about 6.0 mA cm^{-2} (Fig. 4, curve d). The ratio of the current densities of the peaks at 0.12 and about 0.5 V is 2.77. It was reported that the electrooxidation of formic acid could undergo through two parallel pathways, the direct pathway and CO pathway [3,8–13]. The direct pathway is the perfect pathway, because for the direct pathway, formic acid is directly oxidized to CO_2 and no CO intermediate is formed. Thus, the catalyst is not easy to be poisoned. It was also reported that the oxidation of formic acid at the Pd catalyst is mainly through the direct pathway [20,21]. Thus, the current density of the peak at 0.12 V (through the direct pathway) is much larger than that at about 0.5 V (through the CO pathway) at the Pd/C catalyst electrode.

The potentials of the main anodic peaks of formic acid at the Pd–Ir/C catalyst electrodes are almost the same, 0.07 V, which is about 50 mV more negative than that at the Pd/C catalyst electrode. However, the current densities of the main anodic peak of formic acid are different at the different Pd–Ir/C catalyst electrodes. They are 13.04, 16.49 and 18.79 mA cm^{-2} at the Pd–Ir/C-1, Pd–Ir/C-3 and Pd–Ir/C-5 catalyst electrodes, respectively, indicating that the electrocatalytic activity of the Pd–Ir/C-5 catalyst for the oxidation of formic acid is highest among all the catalysts. Because the average sizes of the Pd–Ir particles in the Pd–Ir/C-1 and Pd–Ir/C-3 catalysts are smaller than that in the Pd–Ir/C-5 catalyst, the above results illustrated that Ir in the Pd–Ir/C-5 catalyst could cause the negative shift of the potential of the main anodic peak of formic acid and the increase in the current density of this peak at the Pd/C catalyst. However, Ir does not cause such changes of the peak at 0.5 V (Fig. 4, curves d and c). The ratio of the current densities of the peaks at 0.12 and about 0.5 V at the Pd–Ir/C-5 catalyst electrode is 3.12, which is larger than that at the Pd/C catalyst electrode (2.77). The results illustrated Ir would promote the oxidation of formic acid at the Pd catalyst through the direct pathway.

Fig. 5 displays the linear sweeping voltammograms of the adsorbed CO in 0.5 M H_2SO_4 solution at the different catalyst electrodes. It was observed that no anodic peak appears in the linear sweeping voltammogram at the Ir/C catalyst electrode (Fig. 5, curve e), indicating that CO cannot be adsorbed on the Ir surface. At the Pd/C catalyst electrode, a strong anodic peak of adsorbed CO is located at 0.75 V, illustrating that CO can be strongly adsorbed on the Pd surface. At the Pd–Ir/C-5 catalyst electrode, the anodic peak of the adsorbed CO is located at 0.54 V (Fig. 5, curve c), which is 0.21 V more negative than that at the Pd/C catalyst electrode, indicating that even small amount of Ir exists in the Pd lattice, the adsorption strength of CO on Pd would be significantly decreased. When the content of Ir in the Pd–Ir/C catalyst is increased, the potential of the oxidation peak of the adsorbed CO does not changed, but the current density of the anodic peak is decreased, suggesting that the increase in the content of Ir in the Pd–Ir/C catalyst does not change the adsorption strength, but changes the adsorption amount of CO (Fig. 5, curves a and b).

The above results illustrated that Ir can promote the oxidation of formic acid at Pd though the direct pathway because Ir can decrease the adsorption strength of CO. However, when the content of Ir in the Pd–Ir/C catalyst is high the electrocatalytic activity of the Pd–Ir/C catalyst would be decreased because Ir has no electrocatalytic activity for the oxidation of formic acid. Only when the atomic ratio of Pd and Ir is suitable, the electro-

catalytic activity of the Pd–Ir catalyst can be better than that of the Pd/C catalyst.

4. Conclusions

In conclusion, the Pd–Ir/C catalyst with a small average size and low relative crystallinity of the Pd–Ir particles can be prepared with a very simple chemical reduction method at room temperature. When the atomic ratio of Pd and Ir is suitable the electrocatalytic activity of the Pd–Ir/C catalyst for the oxidation of formic acid is much better than that of the Pd/C catalyst. For example, the potential of the anodic peak of formic acid at the Pd–Ir/C-5 catalyst is 50 mV more negative than that at the Pd/C catalyst electrode and the peak current density at the Pd–Ir/C-5 catalyst is 13% higher than that at the Pd/C catalyst. This is attributed to that Ir can promote the oxidation of formic acid at Pd through the direct pathway because Ir can decrease the adsorption strength of CO on Pd. However, when the content of Ir in the Pd–Ir/C catalyst is too high the electrocatalytic activity of the Pd–Ir/C catalyst would be decreased because Ir has no the electrocatalytic activity for the oxidation of formic acid.

Acknowledgements

The authors are grateful for the financial support of State Key High Technology Research Program of China (863 Program, 2006AA05Z137, 2007AA05Z143), Nature Science Foundation of China (20433060, 20573057), Fund of Department of Science and Technology of Jiangsu Province (BK2006224), the Natural Science Foundation of the Education Committee of Jiangsu Province (05KJB150061).

References

[1] R. Dillon, S. Srinivasan, A.S. Aricò, V. Antonucci, J. Power Sources 127 (2004) 112.
[2] C. Rice, S. Ha, R.I. Masel, P. Waszczuk, A. Wieckowski, J. Power Sources 111 (2002) 83.
[3] C. Rice, S. Ha, R.I. Masel, A. Wieckowski, J. Power Sources 115 (2003) 229.
[4] Y. Rhee, S. Ha, R. Masel, J. Power Sources 117 (2003) 23.
[5] S. Ha, C. Rice, R.I. Masel, A. Wieckowski, J. Power Sources 112 (2003) 655.
[6] US Code of Federal Regulations, 21 CFR 186.1316, 21 CFR 172.515.
[7] Y.W. Rhee, S. Ha, R.I. Masel, J. Power Sources 117 (2003) 35.
[8] X. Xia, T.J. Iwasita, J. Electrochem. Soc. 140 (1993) 2559.
[9] B. Beden, C. Lamy, in: R.J. Cale (Ed.), Spectroelectrochemistry, Theory and Practice, Plenum Press, New York, 1988 (Chapter 5).
[10] A. Bewick, B. Pons, R. Clark, R. Hester, Heyden, vol. XII, Wiley, London, 1985 (Chapter 1).
[11] T.D. Jarvi, E.M. Stuve, in: J. Lipkowski, P.N. Ross (Eds.), Fundamental Aspects of Vacuum and Electrocatalytic Reactions of Methanol and Formic Acid on Platinum Surfaces, Wiley, New York, 1998 (Chapter 3).
[12] N. Markovic, H. Gaseiger, P. Ross, X. Jian, I. Villegas, M. Weaver, Electrochim. Acta 40 (1995) 91.
[13] R. Parson, T. VanderNoot, J. Electroanal. Chem. 257 (1988) 9.
[14] P.N. Ross, in: J. Lipkowski, P.N. Ross (Eds.), The Science of Electrocatalysis on Bimetallic Surfaces, Wiley, New York, 1998, p. 63.
[15] J. Jiang, A. Kucernak, J. Electroanal. Chem. 520 (2002) 64.
[16] S. Park, Y. Xie, M.J. Weaver, Langmuir 18 (2002) 5792.
[17] J.D. Lovic, A.V. Tripkovic, S.L. Gojkovic, K.D. Popovic, D.V. Tripkovic, P. Olszewski, A. Kowal, J. Electroanal. Chem. 581 (2005) 294.
[18] D. Capon, R. Parsons, J. Electroanal. Chem. 65 (1975) 285.
[19] M. Arenz, V. Stamenkovic, T.J. Schmidt, K. Wandelt, P.N. Ross, N.M. Markovic, Phys. Chem. Chem. Phys. 5 (2003) 4242.
[20] S. Ha, R. Larsen, Y. Zhu, R.I. Masel, Fuel Cells 4 (2004) 337.
[21] S. Ha, R. Larsen, R.I. Masel, J. Power Sources 144 (2005) 28.
[22] R. Larsen, S. Ha, J. Zakzeski, R.I. Masel, J. Power Sources 157 (2006) 78.
[23] A. Hamnett, B.J. Kennedy, Eletrochim. Acta 33 (1988) 1613.
[24] T. Shobha, C.L. Aravinda, P. Bera, L.G. Devi, S.M. Mayanna, Mater. Chem. Phys. 80 (2003) 656.
[25] L.A. Kibler, A.M. El-Aziz, D.M. Kolb, J. Mol. Catal. A: Chem. 199 (2003) 57.
[26] R.S. Jayashree, J.S. Spendelow, J. Yeom, C. Rastogi, M.A. Shannon, P.J.A. Kenis, Electrochim. Acta 50 (2005) 4674.
[27] E. Antolini, F. Cardellini, J. Alloy Compd. 315 (2001) 118.
[28] V. Radmilovic, H.A. Gasteiger, P.N. Ross, J. Catal. 15 (1995) 98.
[29] J.H. White, A.F. Sammells, N. Perovskiteand, J. Electrochem. Soc. 140 (1993) 2167.